

REVIEW

Three-dimensional imaging of thoracic diseases with multi-detector row CT

Junji Ueno¹⁾, Tomoya Murase²⁾, Kazuhide Yoneda²⁾, Tetsuya Tsujikawa²⁾, Shoji Sakiyama³⁾, and Kazuya Kondoh³⁾

¹⁾*Department of Radiologic Technology, School of Health Sciences, The University of Tokushima, Tokushima, Japan ;* ²⁾*Department of Radiology, Tokushima University Hospital, Tokushima, Japan ;* and ³⁾*Department of Oncological and Regenerative Surgery, Institute of Health Biosciences, The University of Tokushima Graduate School, Tokushima, Japan*

Abstract : The benefits of multi-detector row CT (MDCT) relative to single-detector row helical CT are considerable. Multi-detector row CT allows shorter acquisition times, greater coverage, and superior image resolution. These factors substantially increase the diagnostic accuracy of the examination. Three-dimensional (3D) volume data from MDCT provides various unique applications on thoracic diseases. These includes isotropic viewings, use of multiplanar reformation (MPR), maximum and minimum intensity projections (MIP and minIP), and volume rendering performed from external and internal perspectives allowing the user to “fly around” and “fly through” the structures. Recent advances in 3D volume rendering put real-time, interactive virtual reality guidance of the procedures such as bronchoscopy and surgery into practice. *J. Med. Invest.* 51 : 163-170, August, 2004

Keywords : MDCT, three-dimensional imaging, respiratory disease, lung, airway

INTRODUCTION

In the early 1990s, single-detector helical CT made possible three-dimensional imaging of various organs (1-5) but this technique was limited by the time needed to cover the region of interest. Recent advance in helical CT scanners have revolutionized the performance. CT scanners have been introduced with increasing numbers of detector rows, referred to as MDCT or multislice CT. The benefits of MDCT relative to single-detector helical CT are improved temporal resolution, greater longitudinal (Z-axis) coverage, and improved spatial resolution in the Z-axis. The performance of recent 16-detector row CT system with 0.4-second rotation represents a nearly 40-fold improvement as com-

pared with the acquisition speed of single-detector row CT. This improvement enables us to get the image data within a tolerable patient breath-hold duration for reduced image degradation induced by organ motion. These factors provide a useful three-dimensional (3D) volume data for thoracic diseases (6-10). This article discusses clinical applications of three-dimensional imaging of thoracic diseases.

ISOTROPIC IMAGING

With MDCT thinner sections can be acquired faster and with greater Z-axis coverage than with single-detector helical CT scanners. When the slice thickness approaches the pixel size in axial images the term isotropic imaging can be applied. Isotropic imaging implies that the voxels that build up the volume data set are cuboidal in shape. It optimizes the appearances of images reconstructed three dimensionally (Fig.1). The combination of iso-

Received for publication May 27, 2004 ; accepted July 13, 2004.

Address correspondence and reprint requests to Junji Ueno, Department of Radiologic Technology, School of Health Sciences, The University of Tokushima, Kuramoto-Cho, Tokushima 770-8509, Japan and Fax : +81-88-633-9020.

tropic data acquisition and fast rotation time is particularly essential for cardiac applications. With new generation MDCT and optimized helical reconstruction algorithms with electrocardiogram synchronization, cardiac motion artifacts can be reduced, depending on the heart rate of the patient (10, 11).

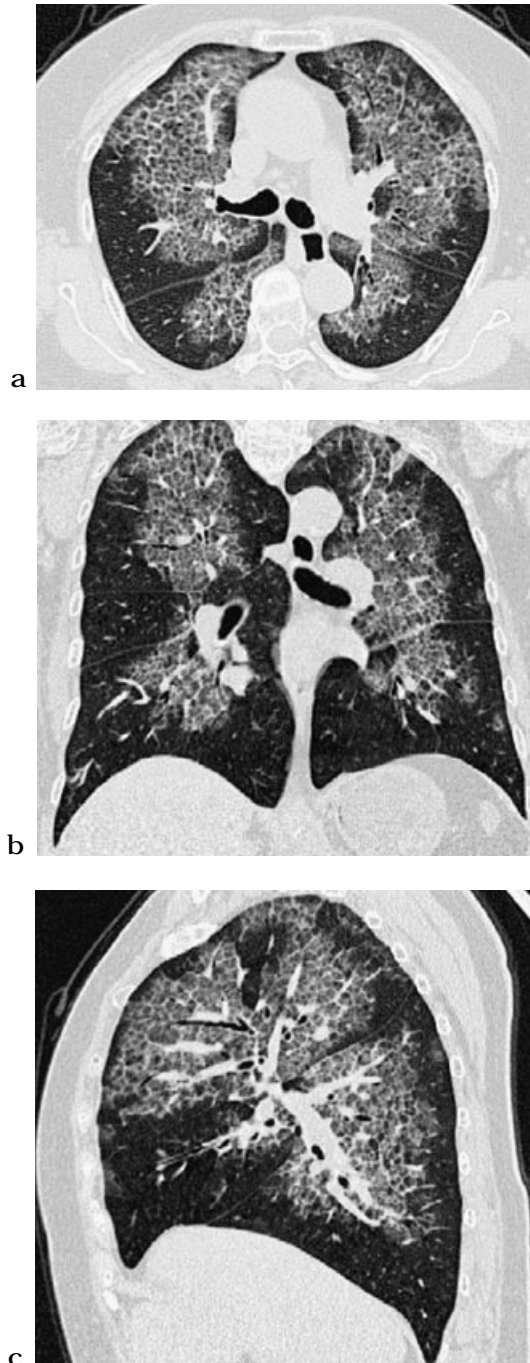


Fig.1-a, b, c
 Isotropic imaging data in multiplanar reconstruction images. In this patient of pulmonary alveolar proteinosis, CT demonstrates areas of patchy ground glass opacification with smooth interlobular and intralobular septal thickening referred to as "crazy paving" (12, 13) in both lungs. Reformatted sectional images (Fig.1-a, b, c) have almost same spatial resolution in all directions. These images are made from a single volume data set from MDCT in a single breath-hold period.

TWO-DIMENSIONAL MULTIPLANAR RECONSTRUCTION (MPR)

The isotropic volume data acquired with MDCT can be displayed in various planes selected two-dimensionally. These two-dimensional reformatted images are generally performed in the coronal and sagittal planes (Fig.2-a). Combination use of three planes, axial, coronal and sagittal, MPR images is essential to interpret a CT study with MDCT. Reformations in oblique and curved planes can also be made, which allow a structure to be traced and displayed as if it lay along a single axis (Fig.2-b, 3, 11-a, 13-b, 14-b, 15-a).

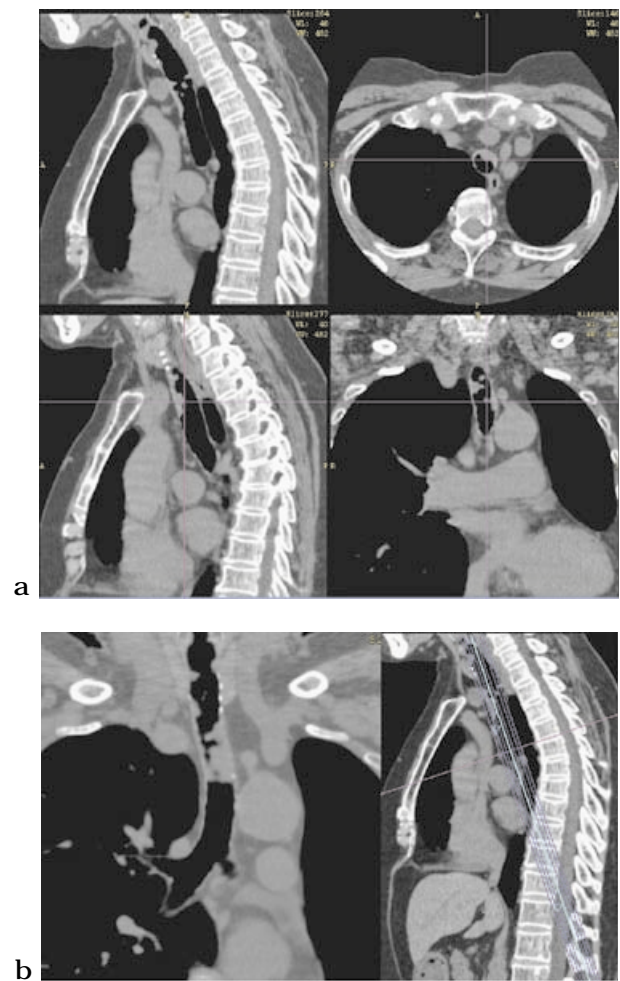


Fig.2-a, b
 Tracheobronchial papillomatosis. Multiple polypoid lesions are seen in the trachea. Original axial images and two-dimensional reformatted images (Fig.2-a) in coronal and sagittal planes are essential to realize the extent of the pathologies and anatomical relationship between the pathologies and adjacent organs. An oblique coronal MPR image along the trachea (Fig.2-b) allows the full length of trachea to be observed. In Fig.2-a, right upper : original axial image, right lower : coronal MPR image, left : sagittal MPR images.

MAXIMUM AND MINIMUM INTENSITY PROJECTION (MIP AND MINIP)

Maximum intensity projection (MIP)(Fig. 4) and minimum intensity projection (minIP) are created in

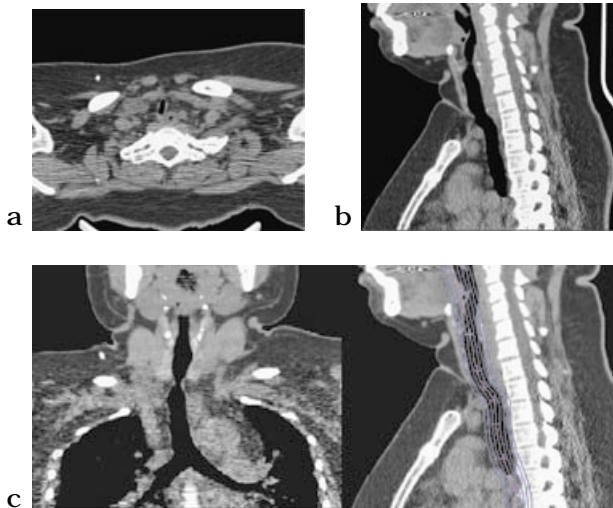


Fig.3-a, b, c
Benign tracheal stenosis. a:original axial image, b:reformatted image in sagittal plane, c : curved MPR image in coronal plane. A benign tracheal stenosis is well demonstrated in the curved MPR image, and the precise sizing of the stenosis can be made with these MPR images.

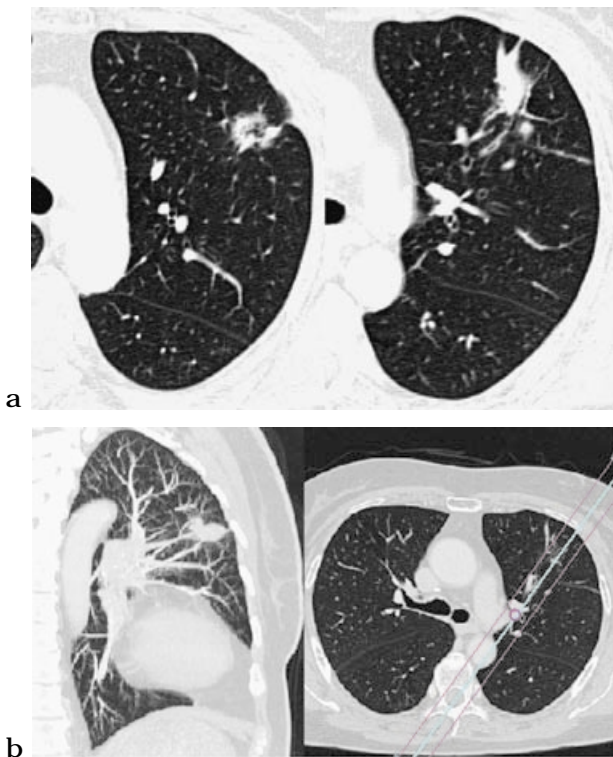


Fig.4-a, b :
Adenocarcinoma of the lung. An irregular shaped mass is seen in left upper lobe, which is proven to be a cancer. Relationship between vasculatures and mass, such as convergence of vasculatures on the mass, is shown to be better advantage with the MIP image (Fig.4-b) compared with conventional axial images (Fig.4-a).

a similar fashion. Those are 3D rendering techniques that evaluates each voxel along a line from the viewer's eye through the volume of the data and selects the maximum voxel value for MIP and the minimum voxel value for minIP. MIP and minIP images have a tendency to misrepresent spatial relationships and limited use in areas overlapping structures. This limitation can be partially overcome with use of sliding slab MIP reconstructions (14). Variable thin slabs can be scrolled interactively through the volume and displayed on a monitor to define anatomic relationship (15). The application of MIP reconstructions for the lung has been shown to increase nodule detection and can help differentiate between small nodules and vessels (Fig. 5)(15). The lumina of airways and emphysematous changes are shown to better advantage with minIP images, which highlights low attenuation structures, such as the air ways and air cysts than with conventional CT images (Fig.6-c)(16).

THREE-DIMENSIONAL VOLUME RENDERING

Volume rendering is generally preferred over surface rendering because of the inherent advantage of displaying the entire range of voxel attenuation values (17). By choosing different parameters, the data can be segmented by attenuation value to display the desired

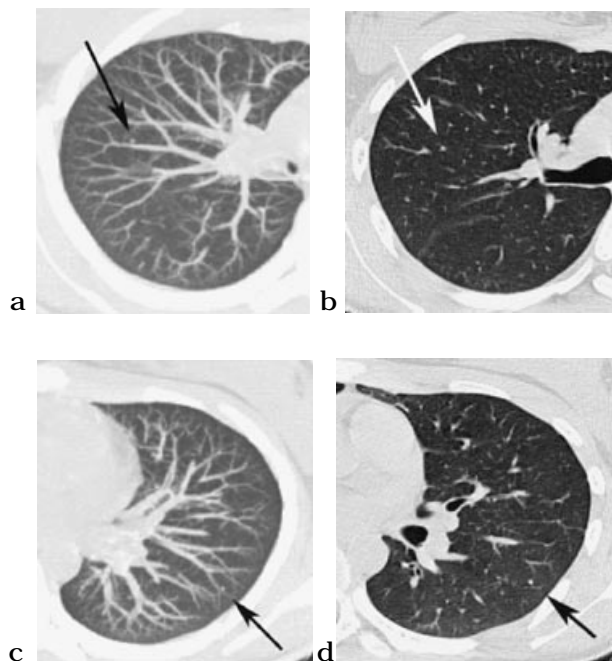


Fig.5-a, b, c, d
Lung metastases. Twenty-millimeter thickness axial MIP images (Fig.5-a, c) are superior to standard axial CT images (Fig.5-b, d) for detecting small pulmonary nodules, because they can help differentiate between small nodules and vessels.

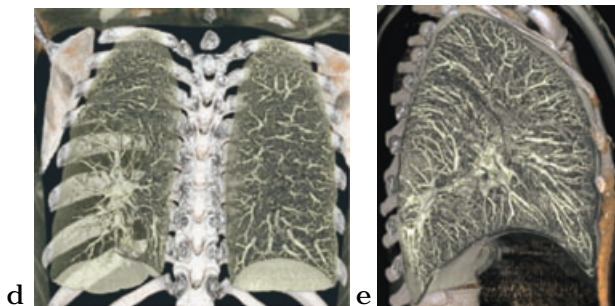
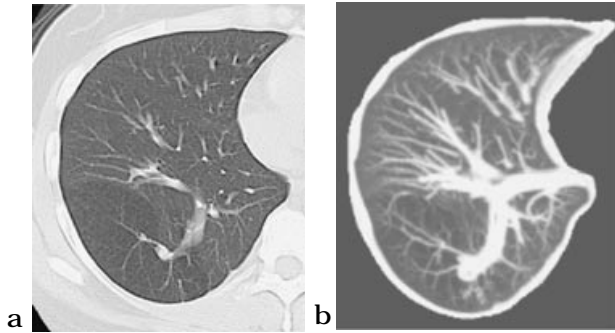


Fig.6-a, b, c, d, e :

An anomaly of pulmonary parenchymal and peripheral vascular development in right lower lobe of the lung. Relationship between vasculatures and anomalous region is shown to be better advantage with the MIP image (Fig.6-b) compared with the conventional axial image (Fig.6-a). The image of minIP (Fig.6-c), which highlights minimum-density voxels such as air-filled structures, is used to enhance visibility of airways. Also note evidence of emphysema. The findings of anomalous broncho-vascular bundles and emphysematous changes are demonstrated with the volume rendering image (Fig.6-d, e).

structure. Volume rendering can be performed from external and internal perspectives allowing the user to 'fly around' and 'fly through' the structures (18) (Fig.7). The endoluminal 'fly through', also referred to as virtual endoscopy, allow the user to navigate through hollow structures in a fashion similar to that of conventional endoscopy. Applications of these 'fly through' and 'fly around' techniques include evaluating airway stenoses, guiding transbronchial biopsies, screening for endobronchial neoplasms, and guiding video assisted

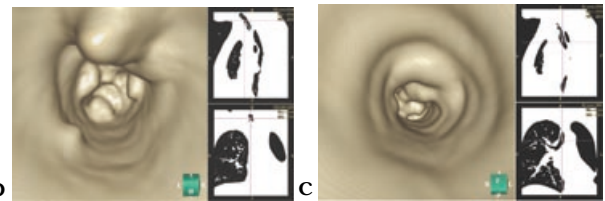
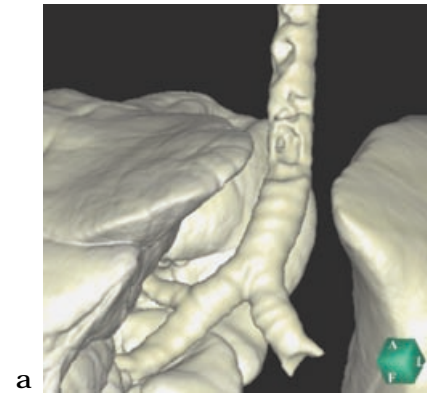


Fig.7-a, b, c :

Tracheobronchial papillomatosis. This is the same patient in Fig.2. Volume rendering images are made from the external (Fig.7-a) and internal (Fig.7-b, c) viewpoints. Multiple polypoid lesions are again seen in the tracheal lumen. The internal rendering, virtual bronchoscopy, can offer the views not only from the proximal portion (Fig.7-b) but also from the portion beyond the site of stenosis (Fig.7-c).

thoracic surgeries (VATS) for lungs. Three dimensional volume rendering can provide a map of relevant anatomy for the surgeon. In VATS the surgical field of view with endoscopic instruments is limited to indirect visualization of a small region, so that preoperative simulation maps with 3D volume rendering play important roles.

APPLICATIONS FOR THE RESPIRATORY SYSTEM (Fig.1-9)

Two-dimensional MPR images facilitate detection of tracheobronchial pathologies. Minimal intensity projection images can also depict the lumina of airways, but clinical utilities are limited in areas overlapping structures. In complex form of stenoses, volume rendering images and virtual endoscopic images are more valuable compared with axial images. The application of thin slab sliding MIP facilitates detection of small nodules and fine linear abnormalities in the lung, because it can help differentiate between diseases and normal bronchovascular structures (Fig.5). Outer perspective images of the lung simulating visceral pleural surface can be made by choosing the attenuation value near the air to be displayed (Fig. 8, 9). Changes in pleural surface affected by pulmonary diseases and nodules

adjacent to the pleura can be seen simulating views in VATS or open surgeries. Applications of volume rendering, fly around and fly through, of the lung and airways are helpful to the surgeon or pulmonologist in planning bronchoscopic or surgical interventions and provide more accurate data for follow-up.

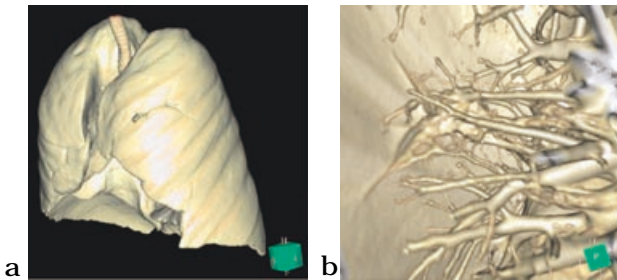


Fig.8-a, b : Adenocarcinoma of the lung. This is the same patient in Fig.6. Volume rendering images simulating the visceral pleural surface can be performed from external perspectives by choosing the threshold, which indicates the air. The pleural retraction to the cancer is well demonstrated (Fig.8-a). The findings of pleural retraction and vascular convergence on the tumor are demonstrated with the volume rendering image from the viewpoint within the lung (Fig.8-b).

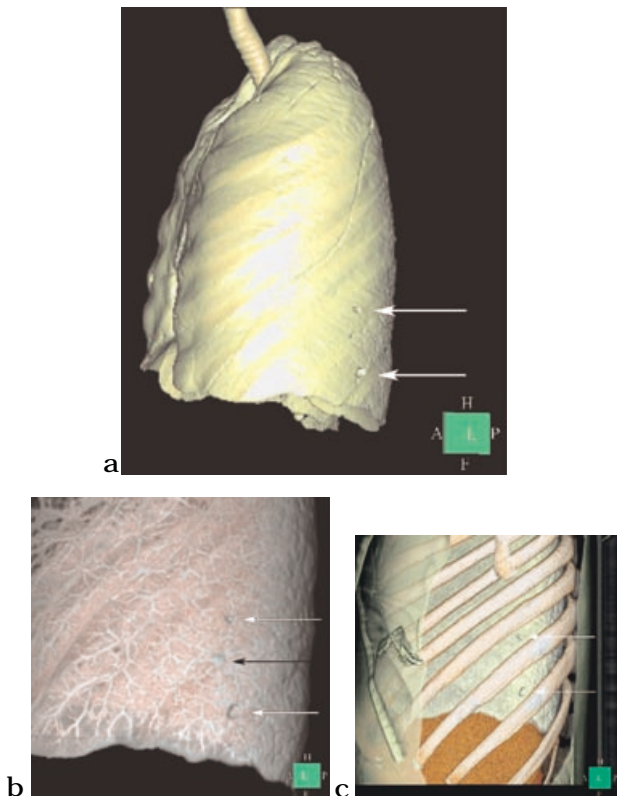


Fig.9-a, b, c : Lung metastases. Small metastatic nodules adjacent to the pleura (white arrows) are seen as small dimpling on the pleura in the volume rendering images (Fig.9-a, b, c). Another small nodule within the lung near the pleura (black arrow) can also be seen by changing the degree of transparency (Fig.9-b). For guiding video assisted thoracic surgeries, the volume rendering image can be made to view the relationship between the rib cage and pulmonary lesions (Fig.9-c).

APPLICATIONS FOR THE CARDIOVASCULAR SYSTEM (Fig.10-14)

The combination of fast gantry rotation time and multidetector-row acquisition become of particular importance for cardiovascular applications. Improved temporal resolution with greater Z-axis coverage enables us to evaluate systemic arteries and veins with non-invasive intravenous contrast medium injection (Fig. 10, 11, 12). Pulmonary arteries can also be evaluated with noninvasive intravenous contrast medium injection (Fig.13). The most exciting advance in cardiovascular imaging with MDCT is noninvasive visualization of the coronary arteries and myocardium (Fig.14)(10, 11). Fast data acquisition capability of MDCT and electrocardiogram synchronization techniques (19) can reduce cardiac motion artifacts. Cardiovascular applications of noninvasive CT angiography contribute to reduce cost and patient radiation dose compare to conventional angiographies.

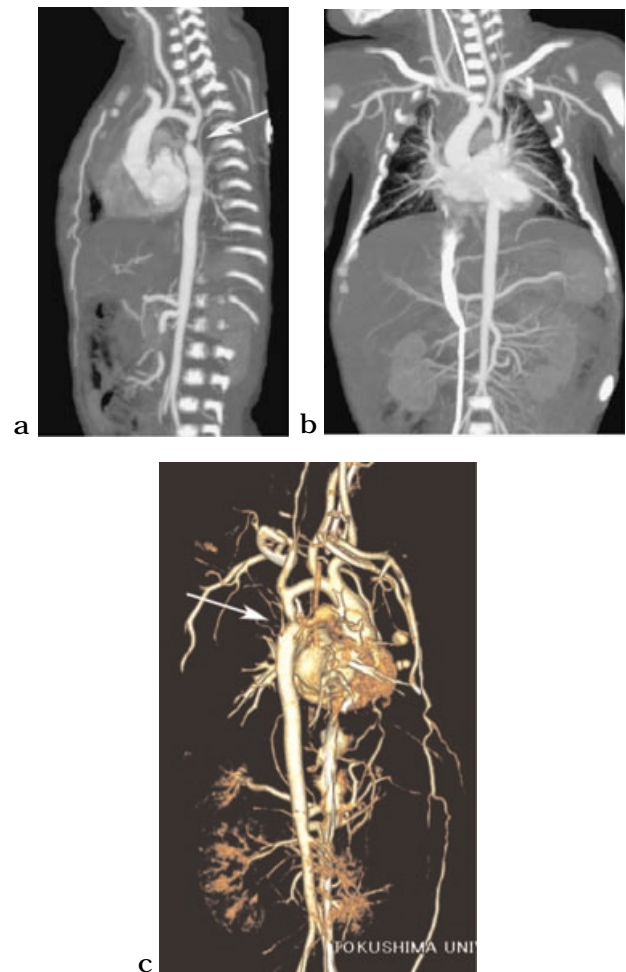


Fig.10-a, b, c : Three-week old patient with aortic coarctation. MIP images (Fig.10-a, b) and VR image (Fig.10-c) show a stenosis (arrow) and characteristic "3" configuration of the aortic arch. Note the enlarged internal mammary arteries.

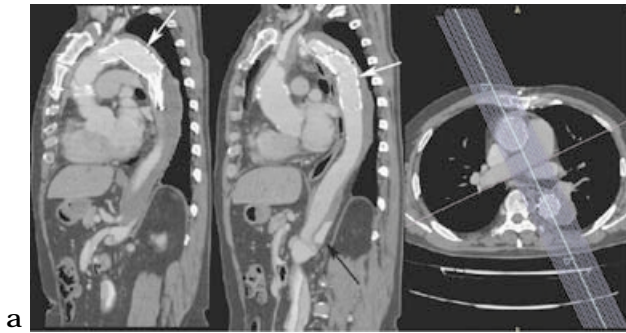


Fig.11-a, b :
 Patient with dissecting aortic aneurysm treated with metallic stents. Combination of conventional axial images and oblique MPR images shows the location and patency of metallic stents (white arrow)(Fig.11-a). Note the false lumen still patent in the abdominal aorta (black arrow). Volume rendering image shows outer perspective of the lumina of the aorta and metallic stents (Fig.11-b).

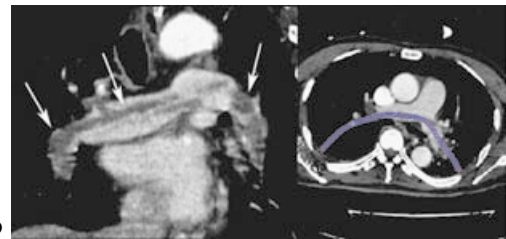


Fig.13-a, b, c :
 Pulmonary embolism. Presence of multiple endoluminal clots on both pulmonary arteries (arrows) are well demonstrated as filling defects in the contrast material-filled right and left pulmonary arteries in the axial CT image (Fig.13-a) and curved MPR image (Fig.13-b). The curved MPR image allows the pulmonary artery to be traced and visualized. Inner perspective of the pulmonary bifurcation viewing from the pulmonary trunk with volume rendering depicts string like clots lying between both pulmonary arteries (Fig.13-c). b-left:curved MPR image, b-right:reference axial image

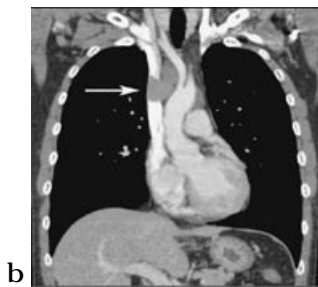


Fig.12-a, b, c
 Thymoma with superior vena cava (SVC) invasion. MPR images (Fig.12-a, b, c) show the lobulated soft tissue mass with small calcifications invading the SVC (white arrows). Note the dilated collateral veins (black arrows) drain into the azygos vein, which connects with the SVC at the point just below the tumor invasion (Fig.12-d, e).

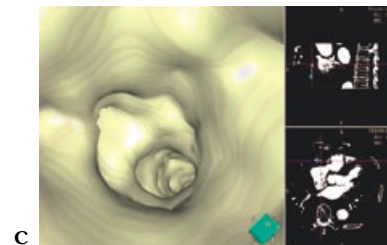
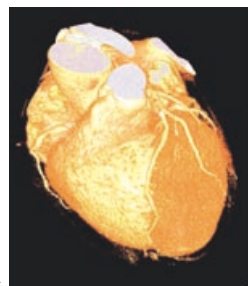


Fig.14-a, b, c :
 Non-invasive coronary arteriogram from the data collected with MDCT using intravenous contrast medium. Volume rendering allows visualization of the right and left anterior descending arteries (Fig.14-a). Curved MPR allows visualization of the course of the left circumflex artery. Note small calcifications of the coronary artery (arrow) (Fig.14-b). Virtual endoscopy can also be applied to the coronary arteries (Fig.14-c).

APPLICATIONS FOR THE CHEST WALL (Fig.15)

Three-dimensional isotropic imaging of bony structures is useful for evaluating fractures, dislocations and deformities of the chest cage (Fig.15). Volume scanning with MDCT assists in the identification of not only bony abnormalities but also soft tissue abnormalities simultaneously, so that in case of traumas MDCT plays important roles (20).

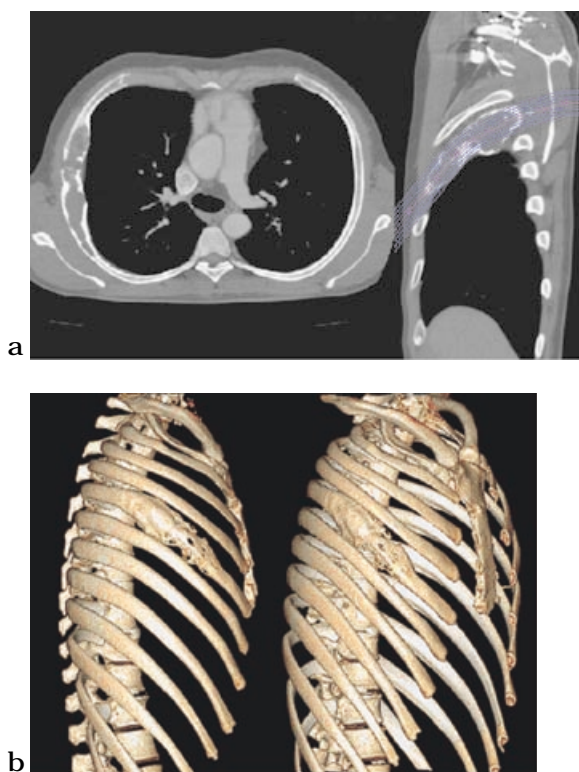


Fig.15-a, b
Fibrous dysplasia of the rib. Curved MPR images allow the rib to be traced and visualized. Note expansion of the rib and endosteal scalloping with thinned cortex of the rib, which is caused by erosion from within. Volume rendering images allow visualization of bony structures well.

CONCLUSION

Multi-detector row CT provides a useful three-dimensional (3D) volume data for thoracic diseases. Three-dimensional volume rendering with real-time and interactive capability of modification of relative pixel attenuation is helpful in detection and perception of thoracic diseases and anatomy. Utilization of 3D images from MDCT is expanding the roles of thoracic CT in various diseases.

ACKNOWLEDGEMENTS

This work was supported in part by a Grant-in-Aid for Scientific Research from Japan Society for the Promotion of Science (15560349). We would like to thank Hiromu Nishitani, MD, PhD, (Department of Radiology, Institute of Health Biosciences, The University of Tokushima Graduate School) for his helpful comments to our works.

REFERENCES

1. Ueno J, Kasem I, Seo K, Higashi T, Yoshida S, Nishitani H : Three Dimensional Longitudinal Dissection view of Hollow Viscus. *NIPPON ACTA RADIOLOGICA* 55 : 76-78, 1994
2. Higashi T, Ueno J, Kasem I, Nishitani H : Three Dimensional Longitudinal Dissection view of the Urinary Bladder. *SCAR* 94 : 729-730, 1994
3. Kasem I, Ueno J, Nishitani H : Diagnostic ability of computer recreated images of pathological lesions of the alimentary system. *SCAR* 94 : 65-66, 1994
4. Nishitani H, Ueno J, Kashihara K, Matsuzaki K, Kasem I : Utilization of Three Dimensional Images in Medicine. *Clinical Image* 11 : 6-12, 1995
5. Ueno J, Nishitani H : Anomalies of pulmonary parenchymal and peripheral vascular development. *INNERVISION* 11 : 49-52, 1996
6. Hu H, He HD, Foley WD, Fox SH : Four multidetector-row helical CT : image quality and volume coverage speed. *Radiology* 215 : 55-62, 2000
7. Rydberg J, Buckwalter KA, Caldemeyer KS, Phillips MD, Conces DJ, Aisen AM, Persohn SA, Kopecky KK : Multisection CT : scanning techniques and clinical applications. *RadioGraphics* 20 : 1787-1806, 2000
8. Lawler LP, Fishman EK : Multi-detector row CT of thoracic disease with emphasis on 3D volume rendering and CT angiography. *RadioGraphics* 21 : 1257-1273, 2001
9. Boiselle PM, Reynolds KF, Ernst A : Multiplanar and Three-Dimensional Imaging of the Central Airways with Multidetector CT. *AJR* 179 : 301-308, 2002
10. Achenbach S, Ulzheimer S, Baum U, Kachelrieß M, Ropers D, Giesler T, Bautz W, Daniel WG, Kalender WA, Moshage W. Noninvasive coronary angiography by retrospective ECG-gated multislice spiral CT. *Circulation* 102 : 2823-2828, 2000
11. Desjardins B, Kazerooni EA : ECG-Gated Cardiac CT. *AJR* 182 : 993-1010, 2004

12. Murch CR, Carr DH : Computed tomography appearances of pulmonary alveolar proteinosis. *Clin Radiol* 40 : 240-243, 1989
13. Johkoh T, Itoh H, Müller NL, Ichikado K, Nakamura H, Ikezoe J, Akira M, Nagareda T : Crazy-paving Appearance at Thin-Section CT : Spectrum of Disease and Pathologic Findings. *Radiology* 211 : 155-160, 1999
14. Calhoun PS, Kuszyk BS, Heath DG, Carly JC, Elliot k : Three-Dimensional Volume rendering of Spiral CT Data : Theory and Method. *RadioGraphics* 19 : 745-746, 1999
15. Napel S, Rubin GD, Jeffrey RB : STM-MIP : a new reconstruction technique for CT of the chest. *J Comput Assist Tomogr* 17 : 832-838, 1993
16. Bhalla M, Naidich DP, McGuinness G, Gruden JF, Leitman BS, McCauly DI : Diffuse lung disease : assessment with helical CT-preliminary observations of the role of maximum and minimum intensity projection images. *Radiology* 200 : 341-347, 1996
17. Johnson PT, Heath DG, Bliss DF, Cabral B, Fishman EK : Three-dimensional CT: real-time interactive volume rendering. *AJR* 167 : 581-583, 1996
18. Ravenel JG, McAdams HP, Remy-Jardin M, Remy J : Multidimensional imaging of the thorax : practical applications. *J Thoracic Imaging* 16 : 269-281, 2001
19. Ohnesorge B, Flohr T, Becker C, Kopp AF, Schoepf UJ, Baum U, Knez A, Klingenbeck-Regn K, Reiser MF : Cardiac imaging by means of electrocardiographically gated multisection spiral CT : initial experience. *Radiology* 217 : 564-571, 2000
20. Rivas LA, Fishman JE, Munera F, Bajayo DE : Multislice CT in thoracic trauma. *Radiol Clin North Am* 41(3) : 599-616, 2003